# SLOPE STABILITY ANALYSIS DURING GROUND MOTION BY MEANS OF NEW DISCRETE MODEL

by

Tadahiko KAWAI[1)] Norio TAKEUCHI[2)] and Masaaki MITO[3)]

## INTRODUCTION

Recently, needs of massive structure, such as atomic power stations, underground oil tanks, etc., have been increased and more reliable design of such structures is requested considering slip and collapsing process from partical failure to total collapse on the soil.

In this paper, Rigid Body Spring Model (abbreviated. RBSM), which was verified to be practical in the static limit analysis of soil foundations, is applied to the dynamic limit analysis during strong ground motion. In this report, fundamental investigation was carried out in order to establish the reliable method for dynamic analysis of soil foundations.

## FORMULATION OF TWO DIMENSIONAL RBSM

Let's consider two dimensional rigid element as shown in Fig. 1. Rigid displacement field is assumed in each element, whose displacements are given by the displacement (u, v, θ) of the centroid as shown in Fig. 1. Horizontal and vertical displacement function at the arbitary point U(x, y), V(v, y) can be given by following equation.

$$\begin{aligned} U(x, y) &= u + r\{\cos(\alpha+\theta)-\cos\alpha\} \\ V(x, y) &= v + r\{\sin(\alpha+\theta)-\sin\alpha\} \end{aligned} \tag{1}$$

where r is distance from the center of gravity to the arbitary point, α is the angle as shown Fig. 1. In case of the displacement with finite rotation, eq.(1) can be approximated by the following equation.

$$\begin{aligned} U(x, y) &= u-(y-y_G)\theta-(1/2)(x-x_G)\theta^2 \\ V(x, y) &= v+(x-x_G)\theta-(1/2)(y-y_G)\theta^2 \end{aligned} \tag{2}$$

Now, $\theta^{(0)}$ implies rotational displacement in previous stage of loading and incremental displacements are (Δu, Δv, Δθ) at the center of gravity. The component of linear displacement, i.e., $\Delta U^{(1)}$ are given by

$$\begin{aligned} &\Delta U^{(1)} = Q\cdot\Delta u \\ &(\Delta U^{(1)})^t = \lfloor \Delta U^{(1)}, \Delta V^{(1)} \rfloor \\ &\Delta u^t = \lfloor \Delta u, \Delta v, \Delta\theta \rfloor \end{aligned} \tag{3}$$

$$Q = \left[\begin{array}{c|c|c} 1 & 0 & -(y-y_G)-(x-x_G)\theta^{(0)} \\ \hline 0 & 1 & (x-x_G)-(y-y_G)\theta^{(0)} \end{array}\right]$$

---

1) Professor, Institute of Industrial Science, University of Tokyo,
2) Director, International Technology Center
3) Penta Ocean Const. Corp. LTD.

Similary the components of nonlinear displacements $\Delta U^{(2)}$ are given by the following vectors.

$$
\begin{aligned}
(\Delta U^{(2)})^t &= \lfloor \Delta U^{(2)},\ \Delta V^{(2)} \rfloor \\
\Delta U^{(2)} &= (1/2)\Delta u^t \cdot N_1 \cdot \Delta u \\
\Delta V^{(2)} &= (1/2)\Delta u^t \cdot N_2 \cdot \Delta u
\end{aligned}
\tag{4}
$$

$$
N_1 = \left[\begin{array}{c|c|c} 0 & 0 & 0 \\ \hline 0 & 0 & 0 \\ \hline 0 & 0 & -(x-x_G) \end{array}\right] \qquad N_2 = \left[\begin{array}{c|c|c} 0 & 0 & 0 \\ \hline 0 & 0 & 0 \\ \hline 0 & 0 & -(y-y_G) \end{array}\right]
$$

Next, consider two adjacent elements ① and ② as shown in Fig. 2 and then the components of linear relative displacement at the point P, $\Delta\delta^{(1)}$ are given by the following equation.

$$
\Delta\delta^{(1)} = \Delta U_2^{(1)} - \Delta U_1^{(1)} \tag{5}
$$

Therefore, substituting eq.(3) to eq.(5), the following equation can be derived.

$$
\begin{aligned}
\Delta\delta^{(1)} &= B \cdot \Delta u \\
(\Delta\delta^{(1)})^t &= \lfloor \Delta\delta_x^{(1)},\ \Delta\delta_y^{(1)} \rfloor \\
(\Delta u)^t &= \lfloor \Delta u_1,\ \Delta v_1,\ \Delta\theta_1,\ \Delta u_2,\ \Delta v_2,\ \Delta\theta_2 \rfloor
\end{aligned}
\tag{6}
$$

$$
B = \left[\begin{array}{cc|c|cc|c} -1 & 0 & (y-y_{G1})+(x-x_{G1})\theta_1^{(0)} & 1 & 0 & -(y-y_{G2})-(x-x_{G2})\theta_2^{(0)} \\ \hline 0 & -1 & -(x-x_{G1})+(y-y_{G1})\theta_1^{(0)} & 0 & 1 & (x-x_{G2})-(y-y_{G2})\theta_2^{(0)} \end{array}\right]
$$

Similary the components of nonlinear relative displacement $\Delta\delta^{(2)}$ can be given.

$$
\begin{aligned}
\Delta\delta^{(2)} &= \Delta U_2^{(2)} - \Delta U_1^{(2)} \\
(\Delta\delta^{(2)})^t &= \lfloor \Delta\delta_x^{(2)},\ \Delta\delta_y^{(2)} \rfloor \\
\Delta\delta_x^{(2)} &= \Delta U_2^{(2)} - \Delta U_1^{(2)} \\
\Delta\delta_y^{(2)} &= \Delta V_2^{(2)} - \Delta V_1^{(2)}
\end{aligned}
\tag{7}
$$

Next, acceleration of rigid element are ($\ddot{u}$, $\ddot{v}$, $\ddot{\theta}$) at the center of gravity and angular velocity is $\dot{\theta}$. Then horizontal and vertical accelerations with finite rotation $\ddot{U}(x, y)$, $\ddot{V}(x, y)$ are given by the following equations.

$$
\begin{aligned}
\ddot{U}(x,y) &= \ddot{u} - (y-y_G)\ddot{\theta} - (x-x_G)(\dot{\theta})^2 \\
\ddot{V}(x,y) &= \ddot{v} + (x-x_G)\ddot{\theta} - (y-y_G)(\dot{\theta})^2
\end{aligned}
\tag{8}
$$

Eq.(8) can be written in the following matrix form.

$$
\begin{aligned}
\Delta\ddot{U}^{(1)} &= H_1 \Delta\ddot{u} + H_2 \Delta\dot{u} \\
(\Delta\ddot{U}^{(1)})^t &= \lfloor \Delta\ddot{U}^{(1)},\ \Delta\ddot{V}^{(1)} \rfloor \\
\Delta\ddot{u}^t &= \lfloor \Delta\ddot{u},\ \Delta\ddot{v},\ \Delta\ddot{\theta} \rfloor \\
\Delta\dot{u}^t &= \lfloor \Delta\dot{u},\ \Delta\dot{v},\ \Delta\dot{\theta} \rfloor \\
\Delta\ddot{U}^{(2)} &= \Delta\dot{u}^t \cdot N_1 \cdot \Delta\dot{u} \\
\Delta\ddot{V}^{(2)} &= \Delta\dot{u}^t \cdot N_2 \cdot \Delta\dot{u}
\end{aligned}
\tag{9}
$$

$$H_1 = \left[\begin{array}{c|c|c} 1 & 0 & -(y-y_G) \\ \hline 0 & 1 & (x-x_G) \end{array}\right]$$

$$H_2 = \left[\begin{array}{c|c|c} 0 & 0 & -2(x-x_G)\dot{\theta}^{(0)} \\ \hline 0 & 0 & -2(y-y_G)\dot{\theta}^{(0)} \end{array}\right]$$

Spring constants assuming on the interelement can be determined in the following way. In case of the isotropic elastic materials the stress-relative displacement matrix $\mathbb{K}'$ is given by

$$\begin{aligned} \sigma' &= k' \cdot \delta' \\ (\sigma')^t &= \lfloor \sigma_n , \tau_s \rfloor \\ (\delta')^t &= \lfloor \delta_n , \delta_s \rfloor \end{aligned} \qquad (10)$$

$$k' = \begin{bmatrix} k_n & 0 \\ 0 & k_s \end{bmatrix}$$

$$k_n = \frac{(1-\nu)E}{(1-2\nu)(1+\nu)} \frac{1}{h_1 + h_2}$$

$$k_s = \frac{E}{(1+\nu)} \frac{1}{h_1 + h_2}$$

where $\sigma_n$ and $\tau_s$ are normal and tagential stress on the interelement boundary. $\delta_n$, $\delta_s$ are also normal and tangential relative displacements. h is the projected length of a vector connecting centroids along the normal drawn. Spring matrix with the global coordinate system is derived by the following matrix equation.

$$k = T^t \cdot k' \cdot T \qquad (11)$$

T is a coordinate transformation matrix. For determination of spring constants in plastic range, plastic flow rule is adopted. Based on the plastic flow rule, the relation between stress increments $\Delta\sigma$ and displacement increments $\Delta\delta$ can be finally obtained in the following form.

$$\Delta\sigma = \left[ k^{(e)} - \frac{[k^{(e)}]\{\partial f/\partial\sigma\}\{\partial f/\partial\sigma\}^t [k^{(e)}]}{\{\partial f/\partial\sigma\}^t [k^{(e)}]\{\partial f/\partial\sigma\}} \right] \Delta\delta \qquad (12)$$

Where f is the plastic potential in the flow theory of plasticity.

With such preliminaries, the following incremental form of the vitrtual work equation can be derived for the dynamic problems.

$$\begin{aligned} &\sum_e \int_{S_b} \delta(\delta^{(0)} + \Delta\delta)^t \cdot (\sigma^{(0)} + \Delta\sigma) ds \\ &- \sum_e \int_A \delta(U^{(0)} + \Delta U)^t \cdot \{(P^{(0)} + \Delta P) - (r/g)(\ddot{U}^{(0)} + \Delta\ddot{U} + \ddot{U}_g{}^{(0)} + \Delta\ddot{U}_g)\} dA \\ &- \sum_e \int_{S_b} \delta(U^{(0)} + \Delta U)^t \cdot (\bar{T}^{(0)} + \Delta\bar{T}) ds = 0 \end{aligned} \qquad (13)$$

$\ddot{U}g^{(0)}$ implies the acceleration of the ground motion at previous stage of loading and $\Delta\ddot{U}g$ also implies the acceleration of the incremental ground motion. Body force and surface traction are represented by P and f respectively. In derivation eq.(13), the term of higher order products of the incremental displacemenets and accelerations were neglected. Eq.(13) is further transformed into the following equation.

$$\sum_e \int \delta(\delta^{(1)})^t \cdot \sigma^{(0)} ds + \sum_e \int \delta(\delta^{(2)})^t \cdot \sigma^{(0)} ds \tag{14}$$

$$- \sum_e \int_A \int \delta(\Delta U^{(2)})^t \cdot (\mathbb{P}^{(0)} + \Delta \mathbb{P}) dA - \sum_e \int_A \int \delta(\Delta U^{(2)})^t \cdot (\mathbb{f}^{(0)} + \Delta \mathbb{f})$$

$$+ \sum_e \int_A \int \delta(\Delta U^{(1)})^t \cdot (\gamma/g) \cdot \Delta \ddot{U}^{(1)} dA + \sum_e \int_A \int \delta(\Delta U^{(2)})^t \cdot (\gamma/g) \cdot \ddot{U}^{(0)} dA$$

$$+ \sum_e \int_A \int \delta(\Delta U^{(2)})^t \cdot (\gamma/g) \cdot (U_g^{(0)} + \Delta U_g) dA = \Delta \mathbb{F} + \mathbb{R}$$

where

$$\Delta \mathbb{F} = \sum_e \int_A \int \delta(\Delta U^{(1)})^t \cdot \Delta \mathbb{P} dA + \sum_e \int \delta(\Delta U^{(1)})^t \cdot \Delta \mathbb{f} ds \tag{15}$$

$$- \sum_e \int_A \int \delta(\Delta U^{(1)})^t \cdot (\gamma/g) \cdot \Delta \ddot{U}_g \, dA$$

$$\mathbb{R} = - \sum_e \int \delta(\Delta \delta^{(1)})^t \cdot \sigma^{(0)} ds + \sum_e \int_A \int \delta(\Delta U^{(1)})^t \cdot \mathbb{P}^{(0)} dA$$

$$- \sum_e \int_A \int \delta(\Delta U^{(1)})^t \cdot (\gamma/g) \cdot (\ddot{U}^{(0)} + \ddot{U}_g^{(0)}) dA$$

$$+ \sum_e \int_{S_b} \delta(\Delta U^{(1)})^t \cdot \mathbb{f}^{(0)} ds$$

In may not be difficult to derive the following matrix equation in incremental form after some calculations.

$$\mathbb{M} \Delta \ddot{u} + \mathbb{m} \Delta \dot{u} + [\mathbb{K}_d + \mathbb{K}_G + \mathbb{K}_a + \mathbb{K}_g - \mathbb{K}_P - \mathbb{K}_f] \{\Delta u\} = \Delta \bar{\mathbb{F}} + \mathbb{R}$$

$$\Delta \bar{\mathbb{F}} = \Delta \bar{\mathbb{F}}_P + \Delta \bar{\mathbb{F}}_f - \Delta \bar{\mathbb{F}}_g \tag{16}$$

$$\mathbb{R} = - \mathbb{R}_\sigma + \mathbb{R}_P + \mathbb{R}_f - \mathbb{R}_a - \mathbb{R}_g$$

$\mathbb{M}$ is the mass matrix and $\mathbb{m}$ damping matrix. $\mathbb{K}d$ is the stiffness matrix with initial displacement, $\mathbb{k}_q$ the geometric matrix, $\mathbb{K}a$ the matrix with initial accelerations, $\mathbb{K}g$ the matrix with initial ground motions, $\mathbb{K}p$ the matrix with initial body forces and $\mathbb{K}_f$ the matrix with initial forces. Furthermore, $\Delta\mathbb{F}$ is the incremental force vector and $\mathbb{R}$ is unbalance force due to manipulation error in previous stage of loading.

(1) Dynamic analysis of the cantilever beam [2)]

Dynamic analysis of the cantilever as shown in Fig. 3 was calculated in order to check accuracy of the solution for the geometrical nonlinear problems. The uniform loads were applied on the both top and bottom surfaces. The results obtained using this model and others are shown in Fig. 4. Where abscissa is time and ordinate implies $\delta/\ell$.

$\delta$ is the displacement at the top of the beam and $\ell$ is the beam length. ● is the solution obtained using this model, ○ is the solution obtained by Shantaram et al. and the broken line is the those obtained by Bathe et al. The obtained results are in good agreement with those obtained by Shantaram et al.

(2) Dynamic elasto-plastic analysis of untreated slope [3]

The slope shown in Fig. 5 collapsed due to the earthquake which occured in the coasting area of the Izu-Oshima Island on January 14, 1978 and damaged the road down the slope.

Some study was made on the failure mechanism of this disaster. First the stiffness of the soil used in the analysis was obtained from the shear wave velocity and the unit weight. In order to evaluate the strength parameter for the surface layer, i.e. layer number ①, the results of the portable cone-penetration test was conducted and $C = 5tf/m^2$ was obtained. For the layers below the surface, it was considered that the behavior of the soils are elastic.

First initial stress were computed from the static analysis and dynamic analysis were performed in order to obtain the slip lines and time history curves of displacement, velocity, etc. The lateral boundary conditions were considered as the vertically free to move for the static analysis and as the horizontally free to move for the dynamic analysis. Rayleigh's damping parameter was calculated by assuming that the 1st and 2nd damping constants are equal to 5%, and increment of the time $\Delta t = 0.01$ sec, and $\beta = 1/4$ for Newmark's $\beta$ method were used for the dynamic analysis. Fig. 5 shows the mesh division used in the analysis and the earthquake wave shown in Fig. 6 was applied horizontally to the base. The maximum acceleration of this wave was 70gal. The actual analysis was performed on the wave of 7 second duration period from 11 sec. to 18 sec. including the maximum acceleration in order to save computation time. In the analysis, maximum acceleration was taken 102 gal. Because it was considered that the acceleration on the road was approximatly 400 gal from the observation of the gravestones overturned and the magnification factor was 4.0.

Fig. 7 shows the results of static analysis. In Fig. 7, the solid line represents the slip line obtained using this model while the broken line represents the real failure line. It can be noticed that at the bottom part of the surface layer the slip line obtained coincides with the failure line.

Fig. 8 shows the slip lines obtained for dynamic analysis. The slip line which already occured at the initial stress state developes along the real failure lines as time passed.

Fig. 9 shows the time history curve of shearing stress and strain, the strain and stress paths with respect to the springs No. 147, 152 and 250. The spring No. 147 away from the failure line shows the elastic response. This is supported by the fact that stress-strain path consist of a straight line. On the other hand the springs No. 152 and No. 250 located near and on the failure line showed existence of the residual strains which indicate the initiation of the slip.

Fig. 10 shows the horizontal and vertical absolute acceleration, relative velocity and relative displacement curves of element No. 107, 111 and 153. The element away from the failure line shows the elastic response while the elements No. 111 and 152 in the sliding soil mass show the residual strains due to the sliding occured. Good agreement is seen between the maximum acceleration measured at the element No. 153 and assumed from the field observation with the value of approximately 400 gal.

Judging from these results, effect of the finite rotational displacement was hardly observed in the present analysis because response displacements were small.

## CONCLUSION

First static analysis of the cantilever beam considering finite rotational displacement was performed and was confirmed the accuracy of the present method for the geometrical nonlinear problems.
Furthermore slope stability analysis was performed during ground motion in order to discuss the mechanisum of slope failure.

For the future study the results obtained here will be used to analyze the disaster due to actual earthquake and to predict the earthquake damage.

## ACKNOWLEDGMENTS

The author wishes to express his sincere thanks to Dr. Kazuhiko KAWASHIMA, Public Works Research Institut, the Ministry of construction, for offerring the important data.

## REFERENCES

1) Kawai, T. "New Element Model in Discrete Structual Analysis", Journal of the Society of Naval Architects of Japan, Vol. 141, 1977

2) D. Shantaram, D.R.J. Owen, O.C. Zienkiewicz "Dynamic Transient Behaviour of Two and Three Dimentional Structures Including Plasticity, Large Deformation Effects and fluid Interaction", Earthquake Engineering and Structual Dynamics, Vol. 4, 1976

3) The Japanese Society of Soil Mechanics and Foundation Engineering, "Earthquake Engineering of Soil", Soil and Foundation Engineering Library 24, pp. 137 ∿ pp. 139, 1983

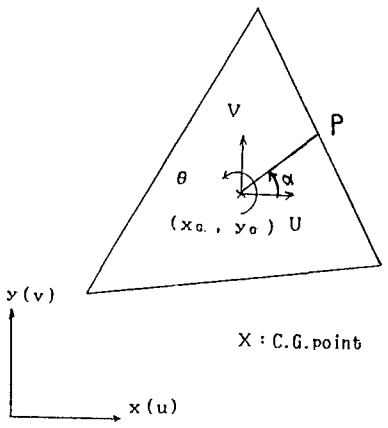


Fig. 1 TRIANGULAR ELEMENT

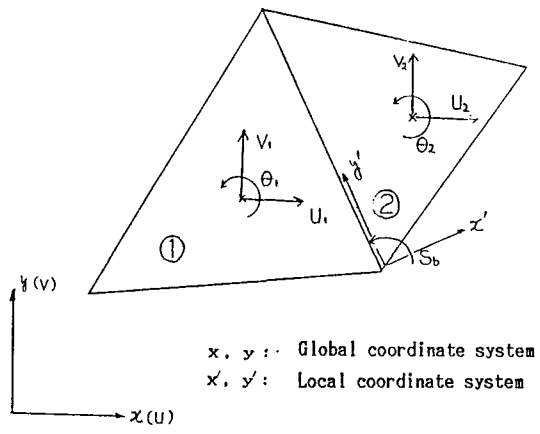


Fig. 2 CONNECTING TRIANGULAR ELEMENENT

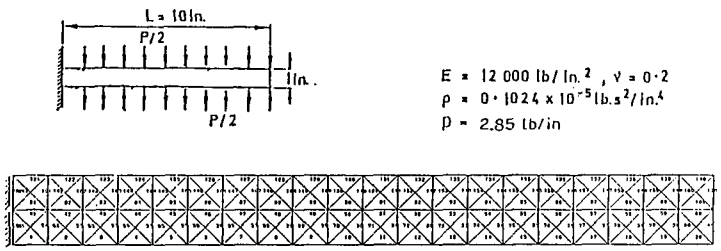


Fig. 3 ANALYSIS MODEL AND MESH DIVISION

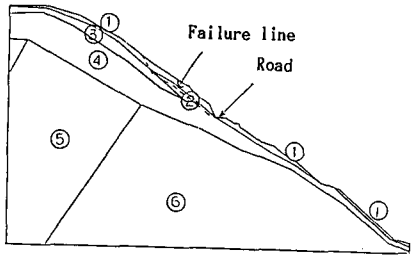


ANALYTICAL MODEL

| | $V_s$ (m/s) | γ (t/m$^3$) | ν |
|---|---|---|---|
| 1 | 160 | 1.7 | 0.3 |
| 2 | 270 | 1.7 | 0.3 |
| 3 | 400 | 2.2 | 0.3 |
| 4 | 620 | 2.2 | 0.3 |
| 5 | 620 | 2.2 | 0.3 |
| 6 | 1320 | 2.2 | 0.3 |

SOIL PROPERTIES

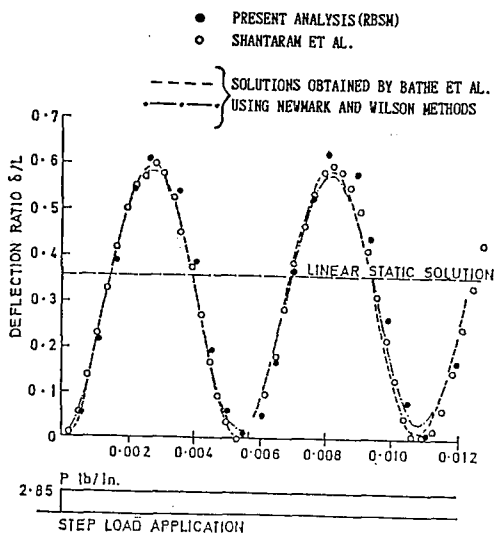


Fig. 4 COMPARISON SOLUTIONS OBTAINED USING RBSM MITH BY SANANTARAM ET AL.

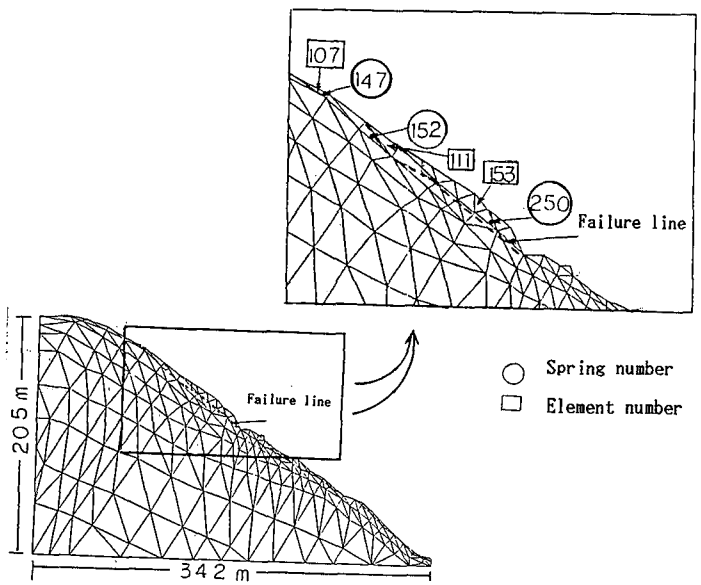


Fig. 5 MESH DIVISION

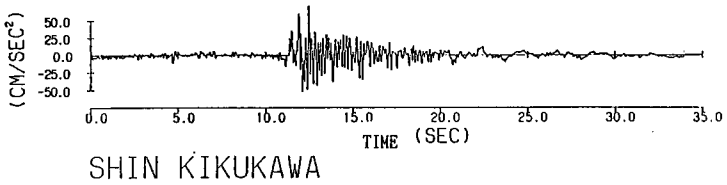


Fig. 6 GROUND MOTION

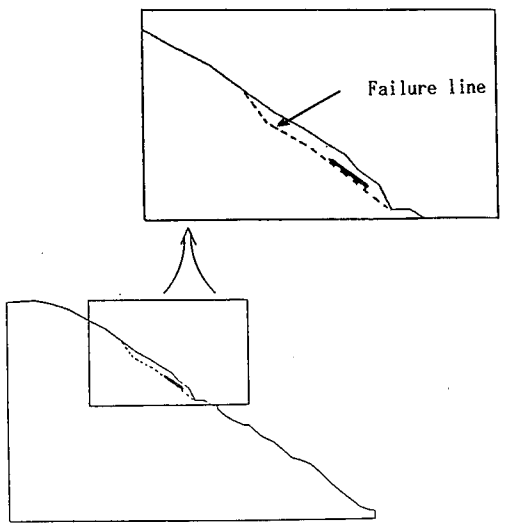


Fig. 7 SLIP LINE AT THE INITIAL STATE

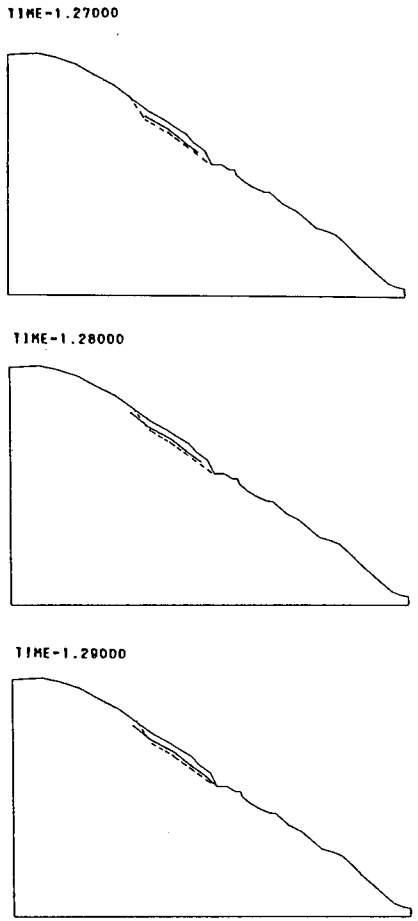


Fig. 8 SLIP LINES WITH DYNAMIC ANALYSIS

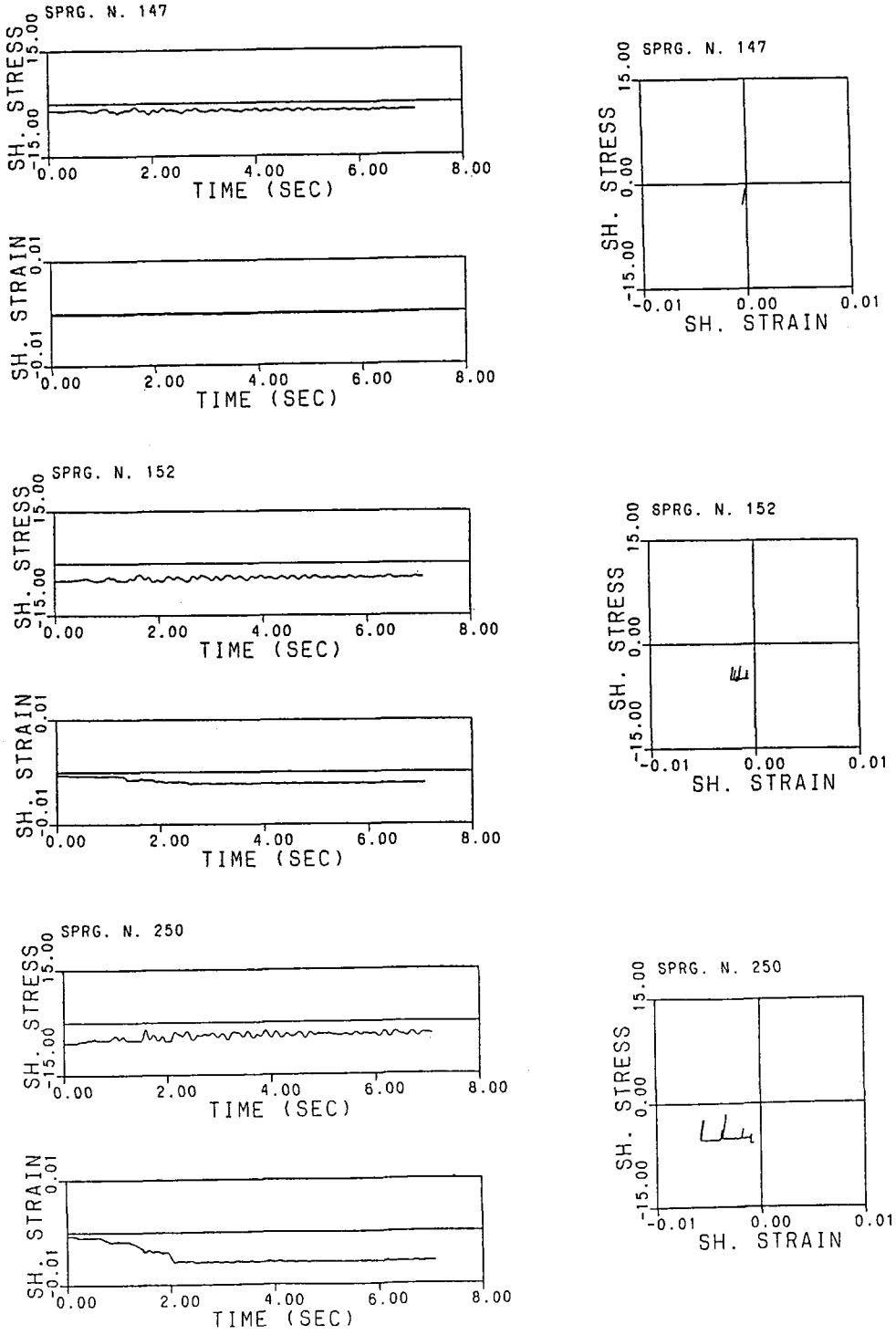


Fig. 9 TIME HISTORY OF SHEAR STRAIN AND STRESS, STRESS AND STRAIN PATH (UNIT ; tf,m)

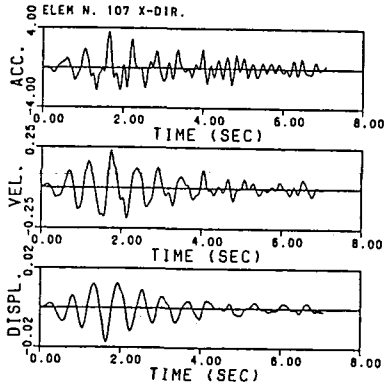


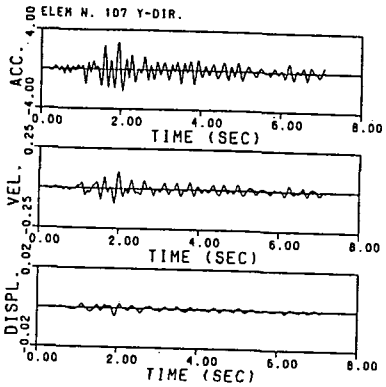


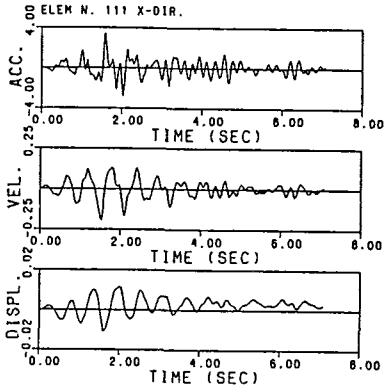


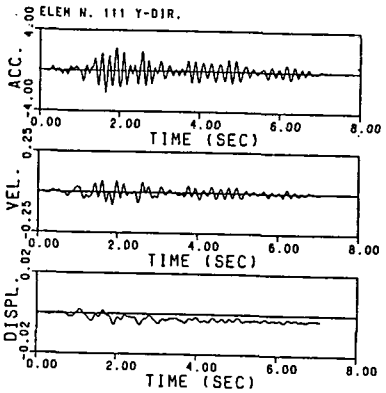


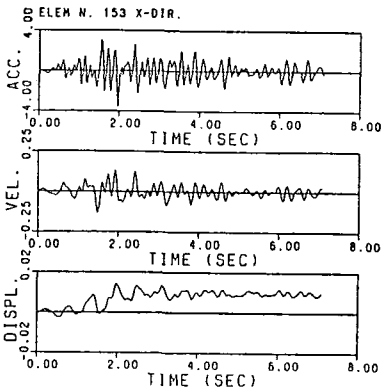


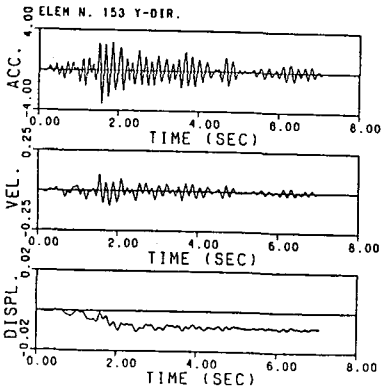


**Fig.10 TIME HISTORY CURVE OF ABSOLUTE ACCELERATION, RELATIVE VELOCITY,RELATIVE DISPLACEMENT (UNIT ; tf,m)**